UNIVERSITY OF TURKU

Two-Dimensional Acoustic Manipulation of Particles in Liquid Media

Department of Mechanical and Materials Engineering

Bachelor's thesis

Author:
Kristofer Kolpakov

13.5.2025

Turku

Kandidaatintutkielma

Tutkinto-ohjelma: Materiaalitekniikka
Tekijä: Kristofer Kolpakov
Otsikko: Two-Dimensional Acoustic Manipulation of Particles in Liquid Media
Ohjaajat: Vipul Sharma, Ph.D., apulaisprofessori ja Kyriacos Yiannacou, Ph.D.
Sivumäärä: 31 sivua
Päivämäärä: 13.05.2025

Ernst Chladni löysi partikkelien käsittelyn akustiikan menetelmin vuonna 1787. Yli 200 vuotta myöhemmin partikkelien akustisen manipulaation sovellukset, kuten niiden ohjaus, kuviointi ja erottelu, ovat yhä ajankohtaisia tutkimuksen kohteita.

Akustinen manipulaatio on menetelmä, jossa akustisia aaltoja käytetään erikokoisten partikkelien liikuttamiseen. Akustiset aallot muodostavat akustisen kentän, joka koostuu painehuipuista ja painepohjista. Akustisen värähtelyn myötä partikkelit liikkuvat poispäin painepohjista ja asettuvat kohti painehuippuja. Partikkelien liikkuminen riippuu niiden ominaisuuksien ja väliaineen välisestä suhteesta. Tällä menetelmällä partikkelit voivat muodostaa monimutkaisia kuvioita. Akustisen värähtelyn vaikutuksesta syntyvät kuviot riippuvat useista tekijöistä, kuten esimerkiksi alustan muodosta, alustan materiaalista sekä ääniaaltojen taajuuksista.

Akustisia kenttiä voidaan hyödyntää myös muihin sovelluksiin, kuten partikkelien erotteluun ja ohjattuun liikuttamiseen. Akustinen erottelu on vakiintunut menetelmä, jota hyödynnetään mikrofluidiikassa. Erottelumenetelmässä yksittäinen painehuippu kanavan keskellä voi erottaa virran partikkeleita ympäröivästä liuoksesta. Erotteluun käytetään antureita, jotka voidaan säätää taajuudeltaan kohdistamaan vain osaa virran partikkeleita. Ohjattu manipulaatio on mahdollista toteuttaa hyödyntämällä konenäköä. Konenäkö havaitsee partikkelit. Konenäön dataa syötetään tämän jälkeen koneoppimismalliin, joka oppii valitsemaan sopivat taajuudet ohjatakseen partikkelit ennalta määrättyä reittiä pitkin.

Opinnäytetyön teoreettisessa osassa esitellään kolme erilaista akustisen manipulaation järjestelmää. Näitä ovat mikrofluidiikan järjestelmä, Chladni-levyn järjestelmä ja ohjatun manipulaation järjestelmä. Tutustutaan myös yleisimpiin akustisiin aaltomuotoihin, joita hyödynnetään lisäksi teoreettisena pohjana työn kokeellisessa osuudessa oman laitteiston rakentamisessa ja tulosten analysoinnissa. Tämän työn kokeellisessa osuudessa kehitetään akustinen manipulaatioalusta ja kuvioidaan polystyreenipartikkeleita akustisella manipulaatiolla.

Kokeiden aikana polystyreenipartikkelien havaittiin muodostavan ruudukkomainen kuvio 107 kHz taajuudella, joka koostui kahdeksasta vaaka- ja pystysuorasta painehuippulinjoista. Lisäksi havaittiin, että painehuippulinjojen määrä noin kaksinkertaistui, kun taajuus kaksinkertaistui. Tämä tulos vastaa aiempia tuloksia kirjallisuudessa. Kokeiden aikana havaitut kuviot eivät olleet säännöllisiä ja symmetrisiä, mikä saattoi johtua peitinlasin ja aluslasin väliin jääneistä ilmakuplista tai aluslasin paikan vaihtelusta.

Aaltotyyppi, joka aiheutti kuvioita työn kokeellisessa mallissa, ei voida varmuudella määrittää ilman jatkotutkimuksia simulaatioilla. Tulosten perusteella voidaan kuitenkin esittää hypoteesi siitä, että kuviot johtuvat heijastuksista ja ohuessa nesteväliainekerroksessa syntyvien seisovien paineaaltojen interferenssistä.

Avain sanat: Akustiikka, Akustinen manipulaatio, Akustofluidiikka, Kuviointi

The originality of this thesis has been checked in accordance with the University of Turku quality assurance system using the Turnitin Originality Check service.

Bachelor's thesis

Subject: Materials Engineering
Author: Kristofer Kolpakov
Title: Two-Dimensional Acoustic Manipulation of Particles in Liquid Media
Supervisors: Dr. Vipul Sharma, Assistant Professor and Dr. Kyriacos Yiannacou
Number of pages: 31 pages
Date: 13.5.2025

Acoustic manipulation as a principle of particle guiding was first discovered in 1787 by Ernst Chladni. Over 200 year later scientists are still investigating the potential of acoustic waves as a means for guiding, patterning and separating particles.

Acoustic manipulation is a technique that can be used to move various sized particles by exciting them with acoustic waves. Acoustic waves create an acoustic field with pressure nodes and antinodes. Due to higher pressure, the particles migrate away from the pressure antinodes and settle on pressure nodes. This movement is dependent on the properties of the particles compared to the hosting medium. This simple principle allows the particles to be moved or patterned into intricate patterns by acoustic excitation. The patterns formed under acoustic excitation depend on several factors such as the shape and material of the substrate and the frequency of the sound waves.

Acoustic fields can also be used for other tasks such as separation and controlled manipulation of particles. Acoustic separation has been commonly used in microfluidic channels where a single pressure node in the middle of a channel can separate a stream of particles from the solution. The transducers used for this separation can be tuned by adjusting their frequency and set to influence a specific set of particles. This effect can be used to effectively separate a mixture of different particles suspended in solution from each other, such as red blood cells from cancer cells. Closed loop manipulation can be achieved through incorporating machine vision to detect the particles and data driven algorithms which, when given a task can over time correctly select the suitable set of frequencies to manipulate the particles along the tasked path.

In this work we focused on fabricating an acoustic manipulation setup based on existing literature and demonstrating its working principle by patterning polystyrene spheres. The first part of the thesis thoroughly breaks down three different acoustic manipulation setups microfluidics-based system, Chladni plate-based system and a feedback-based system. Alongside these three systems we break down some of the most used acoustic wave modes to provide necessary theory for analysing our results and setup.

In our experiments we observed that at 107 kHz polystyrene spheres are patterned into a grid consisting of eight horizontal and vertical lines. Furthermore, we observed that the number of nodes roughly doubles when the frequency is doubled, which matches with the theory that is describe in the analysis chapter. However, the observed patterns were not fully symmetrical nor regular, which was likely caused by small bubbles trapped under the coverslip or the slightly misplaced coverslip on the substrate with the mounted transducers.

After analysing the results of our experiment, we conclude that we cannot confidently determine the dominant waves responsible for patterning in our system without simulation-based validation. However, we hypothesize that the waves responsible for the patterns observed in our experiment are standing pressure waves caused by reflections and interference in the thin fluid suspension layer.

Key words: Acoustics, Acoustic Manipulation, Acoustofluidics, Patterning

List of Symbols and Abbreviations

E	Modulus of Elasticity
v	Poisson's Ratio
ρ	Density
ω	Angular Frequency
λ	Wavelength
f	Frequency
N	Number of Nodes

2D	Two-Dimensional
3D	Three-Dimensional
ARF	Acoustic Radiation Force
BAW	Bulk Acoustic Wave
IDT	Interdigital Transducer
PS	Polystyrene
SAW	Surface Acoustic Wave
SSAW	Standing Surface Acoustic Wave
TSAW	Traveling Surface Acoustic Wave

Table of contents

1 Introduction

The concept of manipulating particles by vibrating them with acoustic frequencies was first discovered by Ernst Chladni in 1787 and published in his work titled "*Entdeckungen über die Theorie des Klanges"*[1]. In his work Ernst Chladni demonstrated that acoustic waves can move particles on rigid plates into intricate patterns now known as Chladni figures. The work of Ernst Chladni has been considered ground-breaking for the field of acoustics and jumpstarted the field of acoustics into its modern state.[1,2]

In recent years acoustic manipulation has yielded several intriguing applications. Acoustic manipulation makes moving, patterning and separating micro- and nanoscale particles with precision possible. Due to the fact that micro- and nanoscale particles are extremely difficult to handle with traditional means, new acoustic manipulation-based methods have been researched and proposed. These methods have been applied to several fields such as drug delivery, nanotechnology, biology and myriad of others.

Exciting a substrate with sound waves can create patterns, which is due to the displacement of particles caused by an acoustic field. These acoustic fields can form standing waves, which consist of antinodes, points of maximum pressure variations and pressures nodes, points of minimal pressure variations. In non-fluidic systems the particles move away from the pressure nodes and settle on the antinodes creating patterns. This is due to the acoustic radiation force (ARF), which causes particles to settle on pressure nodes due to the equilibrium of forces in the acoustic field.[3] In fluid systems the particle migration depends on the acoustic contrast factor Φ. Particles with $\Phi > 0$ such as polystyrene (PS) particles migrate towards pressure nodes while particles with $\Phi < 0$ such as oil droplets migrate to pressure antinodes.[4]

The scope of this work is to fabricate an acoustic manipulation setup based on existing literature and to demonstrate its working principle by patterning PS particles. The overall goal is to understand the working principle of our setup and determine the dominant wave modes responsible for the patterning.

Therefore, the beginning of this work will focus on acoustic manipulation techniques aimed at moving, separating and patterning micro- and nanoparticles. In Chapter 2 we will provide a theoretical overview of the most common acoustic wave modes used in particle manipulation, including surface, bulk and flexural waves. In Chapter 3, we introduce three relevant acoustic manipulation systems that serve as a foundation for our experimental setup. In Chapter 4 we

will describe the design and construction of our acoustic manipulation setup, covering aspects such as signal generation, impedance matching and sample preparation. In Chapter 5 we will present the results of patterning experiments using PS particles. The findings of our experiments will be analysed in Chapter 6, where we compare our observations to theoretical models presented in Chapter 3 and attempt to identify the dominant wave modes responsible for the patterns.

2 Background of Acoustic Manipulation

Acoustic manipulation can be categorized based on the wave propagation modes or the forces exerted on particles. While various propagation techniques exist, this work will focus solely on the most common ones that are applicable to our experimental setup. These include surface acoustic waves (SAWs), which can be further classified into subcategories such as standing surface acoustic waves (SSAWs) and traveling surface acoustic waves (TSAWs). In addition, other propagation modes, including bulk acoustic waves (BAWs) and flexural waves are explored. Figure 1 illustrates four of the wave propagation modes presented in our work excluding flexural waves.

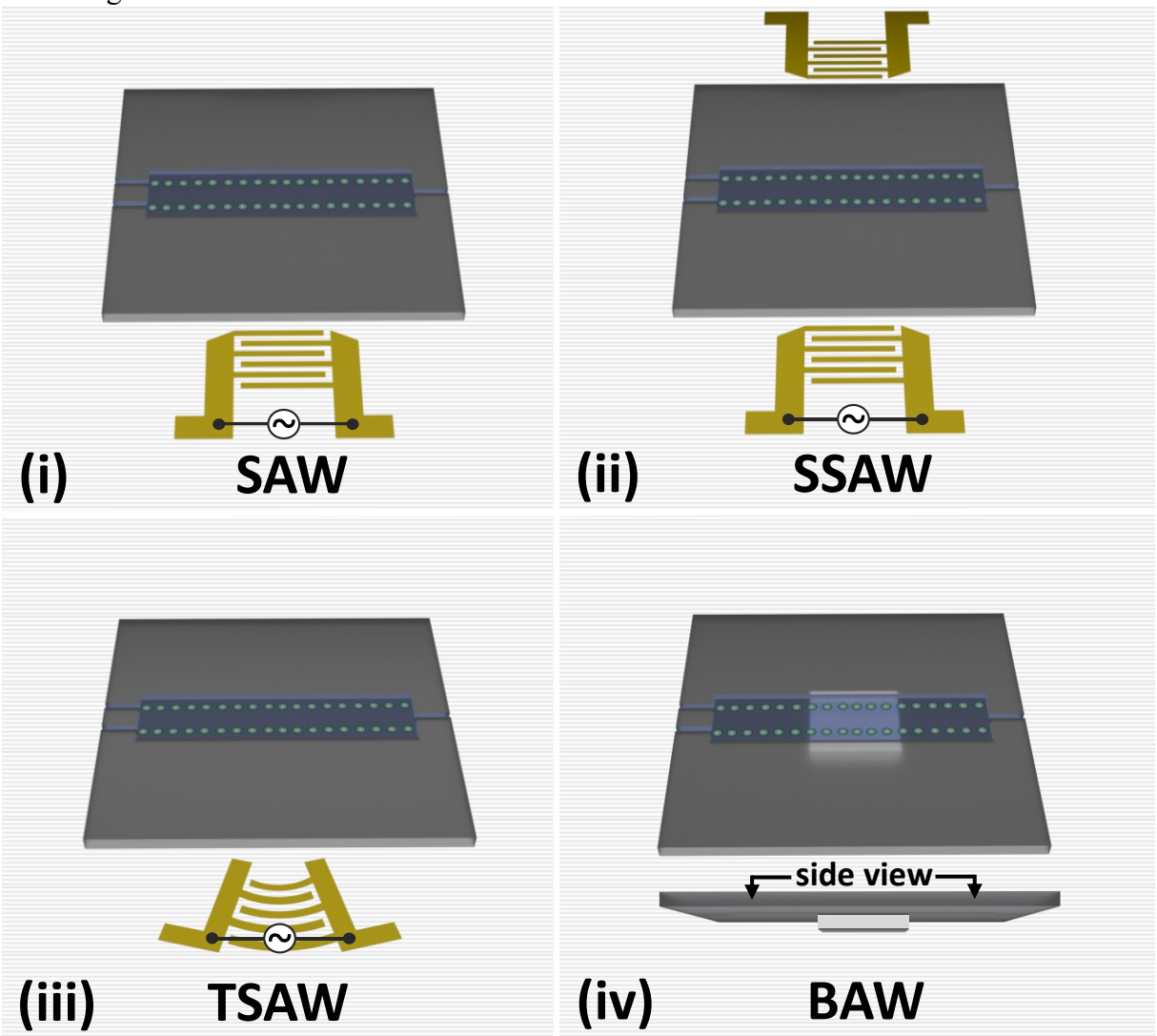

Figure 1. Schematic representation of four wave propagation modes presented in this work. Each image represents a microfluidics channel etched into a plate with particles suspended in liquid. Pressure antinode formed by the sound waves through a specified transducer separate the particles into two columns. (i) SAWs are generated by a single interdigital transducer (IDT). (ii) SSAWs are generated by two opposing IDTs. (iii) TSAWs are generated by a slanted IDT. (iv) BAWs are generated by a bulk ceramic transducer attached to the underside of the plate.

2.1 Surface Acoustic Waves

Surface acoustic waves SAWs also known as Rayleigh waves are elastic acoustic waves that propagate exclusively through the surface of the material. This effectively means that the elastic waves propagate two-dimensionally (2D). Due to their high energy density, SAWs exert a strong ARF on particles, making them effective for patterning particles located on the surface of a material. Consequently, the amplitude decays at a more gradual rate in comparison to other elastic waves, such as bulk acoustic waves (BAWs) where the wave propagates in three dimensions (3D).[5–8]

In acoustic manipulation SAWs are most commonly generated by IDTs, which are patterned electrode structures designed to propagate acoustic waves along piezoelectric surfaces when exited by an alternating current. This is also the case for surface standing acoustic waves (SSAWs) and traveling surface acoustic waves (TSAWs). These two manipulation methods are two of the most common variations of SAW manipulation. While both fall under the broader category of SAW manipulation, they differ primarily in their wave propagation characteristics.[9] An example of a SAW based system is seen in Figure 1 image i, where a gold-coloured IDT is placed in front of a microfluidic channel.

2.2 Standing Surface Acoustic Waves

The location of the acoustic wave source can affect the waves propagating through the system. SSAWs are generated in the case where two transducers produce counter propagating SAWs that interfere constructively and destructively[10,11]. Two opposing transducers create a phase difference. Furthermore, the relationship between the opposing transducers dictates the position of the SAWs on the surface of the substrate. Controlling this relationship allows for precise tweaking and moving of the SSAWs by tuning the transducers.[6] An example of a SSAW based system is seen in Figure 1 image ii, where two gold-coloured IDTs are placed on the opposite ends of a microfluidic channel.

SSAW-based manipulation has been demonstrated in the work of Shi et al. where the opposing IDTs were used to pattern cells one-dimensionally (1D) in a microfluidic channel[12]. In the setup SSAWs responsible for separation can be moved inside the channel by tuning the opposing IDTs[12]. Similar IDT arrangement was used in the work of Chen et al. to align nanowires[11].

2.3 Traveling Surface Acoustic Waves

TSAWs are a variation of SAWs in which a single IDT is oriented perpendicular to the manipulation surface. In this configuration the SAWs generated by the IDT propagate perpendicularly to the direction of the particles' motion. In the works of Destgeer et al. a slanted IDT is positioned perpendicular to a microfluidic channel, causing the SAWs to propagate across the channel and perpendicularly to the flow of particles[13,14]. The use of a slanted IDT enables a broadband TSAW generation[13,14]. An example of a TSAW-based system is seen in Figure 1 image iii, where a gold-coloured slanted IDT is placed in front of a microfluidic channel.

The ARF exerted by TSAWs is significantly weaker than that exerted by SSAWs. For that reason, SSAW manipulation has been much more popular. However, the comparative inefficiency with the use of TSAWs can be circumnavigated through utilizing higher actuation frequencies. Furthermore, many of the techniques and applications revolving around microfluidics such as cell separation, pumping and switching that utilize SSAWs have been demonstrated to be possible with TSAWs. [13,14]

2.4 Bulk Acoustic Waves

BAW-based manipulation is commonly used in microfluidics. BAWs are typically driven by a singular transducer emitting a single frequency or a narrow-frequency band with the channel width being half of the frequency's wavelength.[15] Compared to SAWs where the waves are confined to the surface of a material propagating in 2D, BAWs traverse the entire volume of a substrate propagating in 3D. This volumetric propagation makes BAW-based manipulation excellent for applications involving particles located within the bulk of the material such as microfluidics.[5]

BAWs are typically generated by a ceramic transducer attached to the centre below the manipulation zone or opposite to a second transducer similarly to SSAWs.[15,16] In the work of Augustsson et al. bulk acoustic waves are used in a microfluidic channel to separate two types of cells from each other[16]. The setup uses two pairs of opposing ceramic transducers. The first pair divides the fluid stream into two distinct particle streams, while the second pair separates the cells based on their physical properties.[16] An example of a BAW-based system is seen in Figure 1 image iv, where a grey-coloured bulk ceramic transducer is attached to the underside of a microfluidic channel.

2.5 Flexural Waves

Flexural waves, otherwise known as bending waves or Lamb waves are mechanical vibrations that propagate along thin rigid plates. The behaviour of flexural waves can be described by the Kirchhoff-Love plate equation, which links the wave length to the thickness of the plate. According to Kirchhoff-Love, flexural waves can only efficiently propagate in thin plates when the wavelength of the sound wave is much greater than the thickness of the plate.[10,17,18] When considering flexural waves in thick plates the Mindlin-Reissner plate theory can be applied, which takes transverse shear deformation and rotary inertia into account[19].

The advantage of flexural wave-driven systems is the general cost and the availability of transducers. Flexural wave-based systems can generate waves through the use of piezoelectric transducers, which are inexpensive, readily available and easy to operate in comparison to IDTs.[10] Typically these transducers are attached opposing each other to generate interfering flexural waves. However, flexural waves have also been shown to be achieved with IDTs. One of the most usual applications reported is the aggregation of particles in sessile droplets or in multi-well plates.[17]

2.6 Equations

Capacitive reactance equation for a capacitor in an alternating current circuit. In this study this equation is used to calculate the impedance of a transducer at a specified frequency

$$X_C = \frac{1}{2\pi f C} \tag{1}$$

where X_C is the capacitive reactance in Ω, f is frequency in Hz and C is capacitance in F.[20]

Wavelength equation that describes the relationship between wavelength, wave velocity and frequency universal for all wave phenomenon. In this work this equation is used to calculate the wavelength of the acoustic waves

$$\lambda = \frac{v}{f} \tag{2}$$

where λ is the wavelength in m, v is the speed of sound in m/s and f is the frequency in Hz.[21]

The equation below describes the relationship between the number of acoustic nodes, the length of the acoustic field and the wavelength of the acoustic wave. In this work it is used to estimate the number of nodal lines formed on the manipulation surface

$$N = \frac{2L}{\lambda} \tag{3}$$

where λ is the wavelength in m, N is the number of nodal lines formed on the substrate and L is the distance between two acoustic nodes in m. In this equation it is assumed that the nodes occur at intervals of $\lambda/2$ as is typical with standing waves.[21]

The Kirchhoff-Love phase velocity equation describes the relationship between the material properties of a thin plate and the angular frequency of a flexural wave. In this work, it is used to calculate the velocity of sound for flexural waves

$$v_p = \left(\frac{Eh^2}{12(1-\nu^2)\rho}\right)^{\frac{1}{4}} \cdot \sqrt{\omega} \tag{4}$$

where E is the modulus of elasticity in Pa, h is the thickness of the plate in m, v is the Poisson ratio of the material, ρ is the density of the material in kg/m^3, ω is the angular frequency in (rad/s) and v_p is the velocity of the flexural waves in m/s.[18]

The following inequality defines the geometric validity conditions for the Kirchhoff-Love plate theory. The first inequality ensures that the plate is sufficiently thin for shear deformation and rotary inertia to be negligible. The second inequality ensures that edge effects do not dominate the wave behaviour. In this work it is used to analyse the validity of flexural waves in our setup

$$h \ll \lambda \ll L \tag{5}$$

where λ is the wavelength in m, h is the plate thickness in m and L is the length of the plate in m.[18]

3 Acoustic Manipulation Systems and Applications

For the purposes of understanding the fundamental principles of our setup and the design choices made, we will provide an in depth look at three distinct acoustic manipulation systems. These systems are a Chladni plate system, a microfluidics-based system and a feedback-based system. These systems have served as a foundation for building our own setup. These systems were chosen as the basis for our device, because they utilize similar techniques and fall in line with the results we aimed to achieve.

In the works Zhou et al. the manipulation of micron-sized particles on a thin square plate using flexural waves was demonstrated[2]. Augustsson et al. achieved separation of different cells suspended in liquid in a microfluidic channel with the use of two pairs of opposing ceramic transducers[16]. Similarly in the works of Yiannacou et al. precise feedback-based manipulation of single PS particles and patterning of multiple PS particles using ceramic transducers, with the entire system being driven by machine vision-based algorithm[4,15,22]. Understanding these three systems is helpful, because our setup shares many techniques, design choices and methods used in these systems.

3.1 Chladni Plates

In essence, a Chladni plate is a centrally actuated plate that vibrates. When particles, such as sand or powder are placed on a plate, the sound vibrations cause them to move and arrange into complex patterns along the nodal lines as seen in Figure 2. Thus, by varying the frequency and other parameters such as the shape, thickness and size of the plate different patterns can form.[2,23] Chladni plates can vary in shape, material and dimensions with each property affecting the acoustic field. Thus, by changing the shape of the Chladni plate from a square to a circle, a different Chladni pattern will be achieved. This is due to the fact that the geometry of the plate influences the modes of vibration.[4,24]

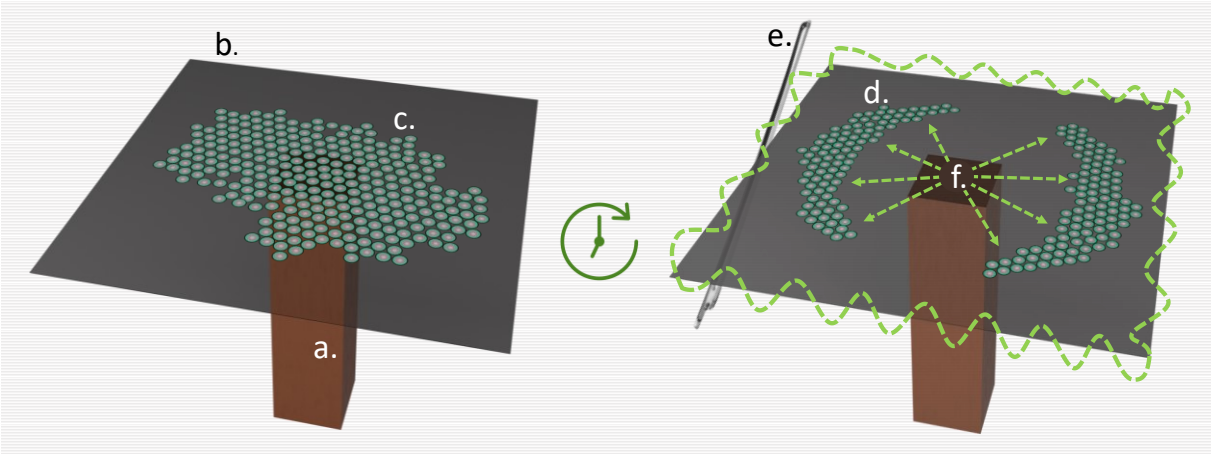

Figure 2. Schematic representation of a Chladni plate before and during acoustic excitation. (a) Central actuator used to vibrate the plate. (b) Thin rigid plate serves as the substrate for particle manipulation. (c) Particles initially distributed randomly across the plate. (d) Particles organized into a distinct pattern under acoustic excitation. (e) Alternatively, the plate can be excited by drawing a violin bow against the edge of the plate making the plate vibrate as in the works of Ernst Chladni[1]. (f) Flexural waves generate pressure nodes and antinodes. Particles are guided towards the pressure nodes.

In the early stages of research related to acoustics, the Chladni plates were exited mechanically by drawing a violin bow at the edge of the plate while holding it as seen in Figure 2. Other excitation methods have included a brass plate and a chisel or a violin bow string. More recently speakers, ceramic stack transducers and piezoelectric transducers have been used as the source of vibration. The position of the vibration source alters the boundary conditions and in return affects the nodal lines formed on the plate.[24]

3.2 Acoustofluidics

Acoustic manipulation has been shown to be extremely promising in the field of microfluidics sparking a myriad of publications and new exciting applications[5]. Microfluidic devices are systems that process or manipulate fluids in nanoscale 10^{-9} and smaller utilizing fluid flow channels with dimensions of tens of micrometers[25]. Figure 3 illustrates an acoustofluidic device used in the work of Augustsson et al. for cell separation. The most common applications for these acoustofluidic devices are analysis, diagnostics and synthesis of chemical and biochemical substances.

When comparing acoustofluidic devices to Chladni plate-based devices, there are two main differences, the presence of a third dimension i.e., the walls of the microfluidic device and the presence of a liquid medium in which the particles are suspended. This means that the properties of the liquid medium should be considered and chosen based on the needs of the device. For example, the speed of sound in water at room temperature is 1497 m/s where as in ethanol 1162

m/s. This difference will affect the formation of the acoustic field as well as the strength of the ARF. Furthermore, since acoustofluidics can utilize 3D, the particles can have a greater freedom of movement and more complex patterns can form.

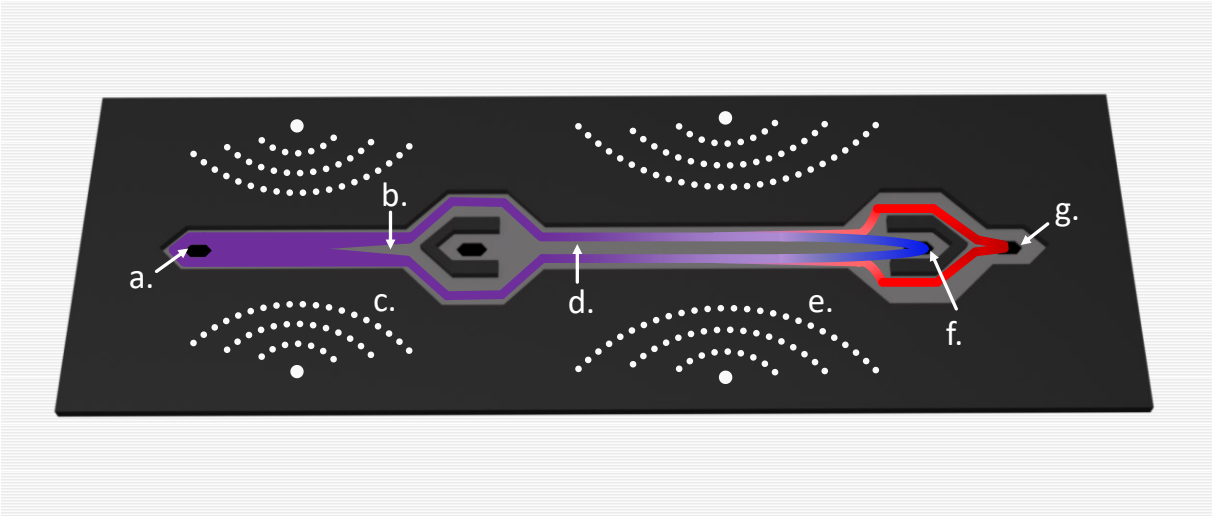

Figure 3. Schematic representation of an acoustofluidic cell separation device. (a) Inlet for unseparated blood. (b) First channel dedicated to cell prealignment. (c) First pair of transducers emitting an ultrasound frequency f_1 = 5 MHz (d) Second channel w_2 = 375 µm dedicated to cell separation. (e) Second pair of transducers emitting an ultrasound frequency f_2 = 2 MHz (f) First outlet serving as an exit point for cancer cells. (g) Second outlet serving as an exit point for blood cells. This image has been reproduced on the basis of Augustsson et al.'s publication.[16]

In the setup of Augustsson et al. the particles are first funneled through an inlet located at the front end of the device[16]. The particles are prealigned into two separate streams in the first channel by an antinode generated by two opposing ceramic transducers. The opposing transducers create an acoustic field (a-a′) in the yz-plane. After the prealignment a second pair of opposing transducers influence the cancer cells towards the first outlet while the healthy red blood cells are naturally flow towards the second outlet effectively separating them from the cancer cells. This principle is based on the fact that the frequency emitted by the second transducer pair only affects the cancer cells while the healthy red blood cells remain unaffected. With this method the cells were separated with purity ranging from 79.6 % up to 99.7 %.[16]

3.3 Feedback-Based Acoustic Manipulation

Feedback-based controlled manipulation is achieved through utilizing acoustic models and adaptive algorithms. After many cycles these models can apply the correct set of frequencies to manipulate particles along a predetermined path. This can be applied to a single or multiple particles.[2,22,23] This can be achieved both in dry form[2,23] and in liquid suspension[4,15,22].

In the works of Yiannacou et al. machine vision-based machine learning is utilized to move particles by reacting to their movement[4,15,22]. The systems described in three publications utilize

an algorithm, which through gathering data over various cycles applies frequencies to move particles along a set path. The movement of the particles caused by excitation is tracked by a camera. The algorithm gathers data on the movement of the particles caused by a frequency and labels them as successful and unsuccessful by assigning each frequency a reward value. This data is then applied to move particles along desired paths through a trial-and-error approach. In these studies, the controllable manipulation is implemented in a microfluidic system, where sound waves generated by transducers can transport particles and droplets as an alternative to mechanical pumps. The particles can be moved in complex paths such as spelling out letters or text. Each cycle has a set path as well as a finish line.[4,15,22]

At each control cycle the algorithm selects a frequency based on the particle response to actuation. This information is gathered by the algorithm through machine vision-based camera that compares the positions of the particles at each excitation cycle. One of the main algorithms used in the work of Yiannacou et al. was labeled ε-greedy, which selected a frequency from a pool of $N = 100$ and a frequency range of 65 kHz to 700 kHz[15]. Figure 4 illustrates the ε-greedy algorithms working principle.

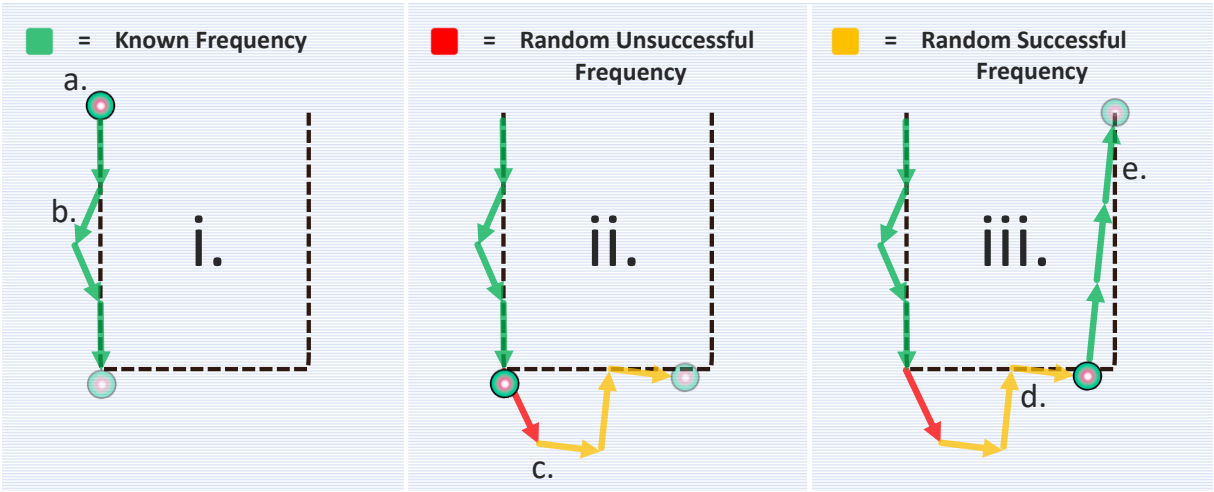

Figure 4. Illustration of the ε-greedy algorithms working principal. (i), (a)The particle is placed at the beginning of the desired path. (b) Algorithm applies a known frequency with the highest reward from the pool N = 100 and a frequency range of 65 kHz to 700 kHz. (ii), (c) When there no known applicable frequencies, the algorithm picks a random frequency from the pool. (iii), (d) Some of the frequencies end up being successful and the data reward values are adjusted. (e) The algorithm frequencies with unassigned reward values to the pool of known frequencies. This image has been produced on the basis of Yiannacou et al.'s publication.[15]

Initially the algorithm uses all the available frequencies to gather information regarding particle movement in relation to applied frequency. Afterwards the algorithm selects frequencies based on past information from which the algorithm applies the frequency with the highest reward. With a probability of ε the algorithm performed a random action i.e., selected a random frequency. In this case the reward correlated to the distance travelled towards the selected point.

If the algorithm could not find a suitable frequency, it reduced the reward of the last used frequency and chose a new frequency with the highest reward. This continued until the algorithm chose a random frequency from the pool that affected the particles position and the algorithm adjusted accordingly. By leveraging past successful actions, the algorithm could determine a suitable frequency to apply and move the particles to the desired location.[15]

4 Methodology

The setup built for this thesis is a part of an ongoing project done as part of the Materials for Flexible Devices group under the supervision of Dr. Vipul Sharma in the department of Mechanical and Materials Engineering University of Turku. For that reason, schematics, description, functionality and purpose of the device is not as of now publicly available information. Thus, the description and details of the setup will be generalized.

4.1 Experimental Setup

Similarly, to many acoustic manipulation setups such in the works of Augustsson et al. and Yiannacou et al. our setup consists of a signal source i.e., a function generator, a radio frequency amplifier and an impedance matching network[15,16]. All of the parts are connected via BNC coaxial cables with the impedance of 50 Ω. To minimize signal reflections and to maintain signal integrity, the lengths of the 50 Ω coaxial cables were kept as short as possible, at the length of 20 cm.

For our setup an arbitrary waveform generator was used to produce continuous sinusoidal signals at the desired operating frequency. The signal was generated using an arbitrary function generator (Keysight 33511B, 20 MHz, 1-channel). This model was picked for its ability to generate arbitrary waveforms and the compatibility with MATLAB. Through the interface with MATLAB any kind of wave could be generated and the experiments could be automated to change parameters such as amplitude, frequency and waveform automatically through a custom MATLAB code. The function generator was limited to a maximum output of 10 Vpp and a frequency bandwidth up to 20 MHz. However, the 10 Vpp output was insufficient for our needs and therefor signal amplification was necessary.

In a typical setting a regular amplifier can be used to amplify the signal. However, a regular amplifier has an insufficient bandwidth making amplifying high frequency signals impossible. To overcome the limitations of a regular amplifier, a radio frequency amplifier was necessary. For our setup we used a radio frequency amplifier (WMA-320 Falco Systems). This radio frequency amplifier provided a fixed gain of ×50 with an output range of ±150 V and a wide bandwidth of DC to 5 MHz. This amplifier was perfectly equipped to amplify capacitive loads, which suited our needs perfectly. Although the amplifier limited our bandwidth to 5 MHz, the ×50 gain was deemed more beneficial that the limitation to the bandwidth.

Our setup operated at an impedance value of 50 Ω. However, the transducers used for the acoustic excitation have a frequency dependant impedance. This can be calculated using Equation 1 and plotted as seen in Figure 5. According to Figure 5, the lower frequencies have a higher impedance and that with the increase in frequency the impedance approaches zero.

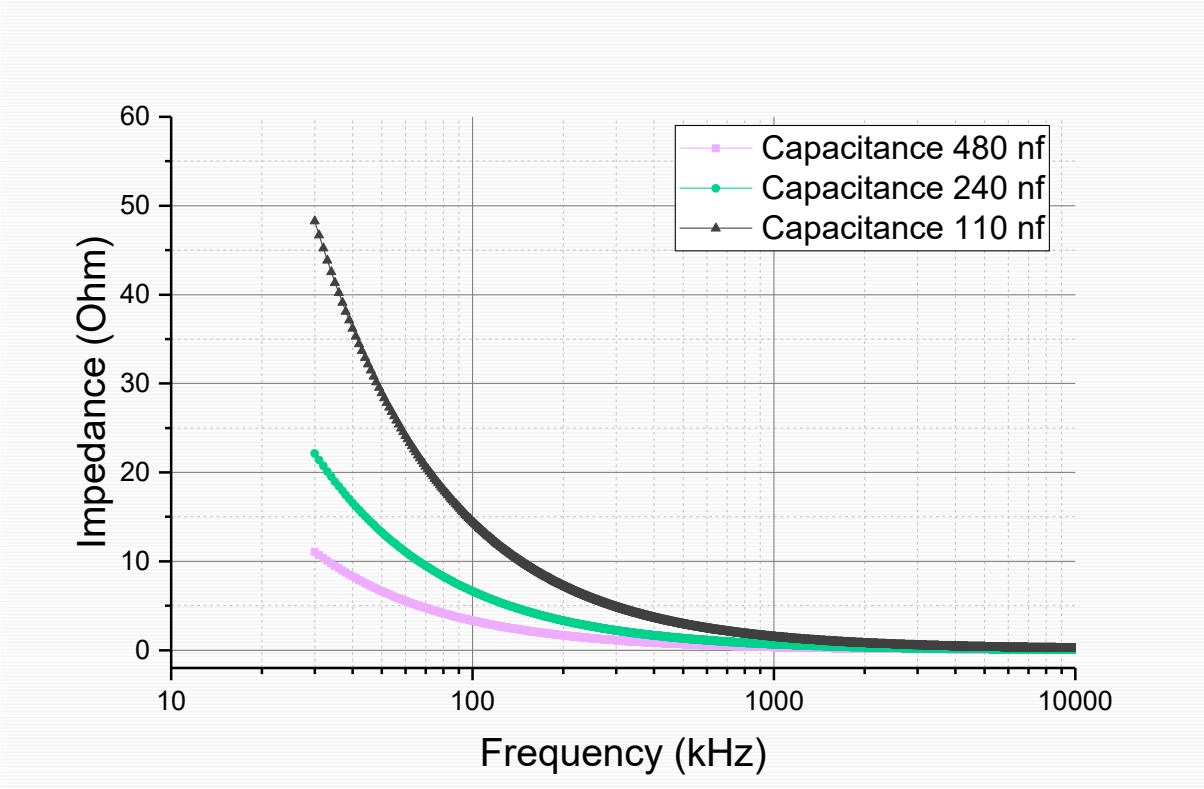

Figure 5. Impedance as a function of frequency for three transducers with different dimensions and capacitance. The pink curve represents the transducer with capacitance of C = 480 nf that was used in the setup and the other two were considered but ultimately not chosen.

Our system operates at a standard impedance of 50 Ω and the impedance of the transducer approaches zero at higher frequencies, which results in an impedance mismatch. Impedance mismatch causes inefficiency in signal transfer between the signal source and the transducers. To address this, we matched the impedance between the signal source and the transducer using a transformer (E&I JT-3, 3.1 Ω matching transformer), which converts the system's 50 Ω output into a 3.1 Ω load.

Using Equation 1 and inputting the capacitance of the transducer that we chose C = 480 nf the frequency at which the impedance of the transducer equals to 3.1 Ω was calculated. This occurs at approximately $f \approx$ 107 kHz at which point the signal source's and transducer's impedance is matched. This enables efficient signal transfer. Consequently, the frequency $f \approx$ 107 kHz was chosen as our starting frequency.

However, if the operating frequency changes, for instance doubled as in our experiments the impedance of the transducer changes disrupting the impedance matching. Even so it is significantly more efficient to transfer a 3.1 Ω load into transducer that operates on a lower impedance than a 50 Ω load.

4.2 Chip Fabrication

In this work the chip is defined as the interface between the substrate, the sample and the coverslip. When the sample is dried between the substrate and the coverslip it leaves a dry pattern. If we would use a conductive material, the dry pattern could act as a chip or a conductive network. The idea of utilizing PS particles in a 2D environment was selected based on the works of Yiannacou et al.[4,15,22]. The attachment of two opposing transducers on the top surface of the substrate and mounting a coverslip on top of the sample creating a makeshift chamber without walls was selected based on the work of Chen et al.[11] In our setup two bulk ceramic transducers (Piezomechanik PCh 150/10 mm × 10 mm × 2 mm) were positioned opposite of each other and driven with the same signal. The transducers were attached to the substrate with epoxy (Power Epoxy, Loctite).

The glass substrate used for our setup was a fused quartz substrate cut according to the following dimensions (75 mm × 75 mm × 2 mm). The substrate was mounted on a 3D printed frame so that the device could be mounted inside the base of an optical microscope. The droplet was placed on the middle of the top surface of the fused quartz substrate after which it was covered by a borosilicate coverslip with the following dimensions (18 mm × 18 mm × ~0.15 mm).

4.3 Sample Preparation and Analysis

The samples were prepared with identical parameters for optimal comparison between frequencies. Same diluted stock solution was used for every sample. To visualize patterns formed by the acoustic fields PS particles (Micro particles based on polystyrene, dark red, 10 μm) suspended in distilled water were used.

To enhance particle dispersion and reduce the surface tension of water, the solution was prepared by mixing polystyrene microbeads, Triton X-100 surfactant and distilled water in a 1:1:8 volume ratio corresponding to 10 % particles, 10 % surfactant and 80 % distilled water in the final mixture. Reducing the surface tension with surfactant enabled the particles to migrate

quicker under acoustic excitation. Furthermore, without surfactant during drying a bubble would form between the substrate and the coverslip collapsing the pattern, which the surfactant prevented.

Each sample equalled to a 25 µl droplet pipetted on the surface of the substrate. The samples were positioned as centrally as possible in relation to the two transducers. Due to pipetting by hand, the position of the droplet varied by several millimetres between samples. After the sample was pipetted, a coverslip was mounted on top of the droplet to disperse the particles, minimize Brownian-motion and limit the particles movement to 2D.

During acoustic manipulation the samples were placed under an optical microscope (Microscope BS.1153-EPL) so that the movement of the particles and the formed patterns could be observed before, during and after the acoustic manipulation. The particles were imaged with a microscope camera (ToupTek Camera, ToupCam E3ISPM 2100A)

5 Results

To demonstrate patterning on our setup we prepared five samples. Besides frequency all of the samples were created using the same parameters of 3 Vpp amplified ×50 and at the impedance of 3.1 Ω. All samples were prepared from a 25 µl droplet of solution containing PS particles, surfactant and distilled water mixed in a 1:1:8 volume ratio. Each sample was acoustically excited for 15 minutes after which images were taken both with a camera and a microscope camera. The first sample was exited at the frequency of 107 kHz after which the following samples were exited at double the frequency of the previous sample.

The results are shown in Figure 6. The patterns were visible under strong illumination such as a microscope light, which was used for the images presented in Figure 6. The microscope images show an extremely zoomed in image making so that seeing the whole pattern is not possible. In these images we are able to see only a small part of the pattern, which becomes more eligible with the increase in frequency. This is due to the pattern becoming thinner and more intricate.

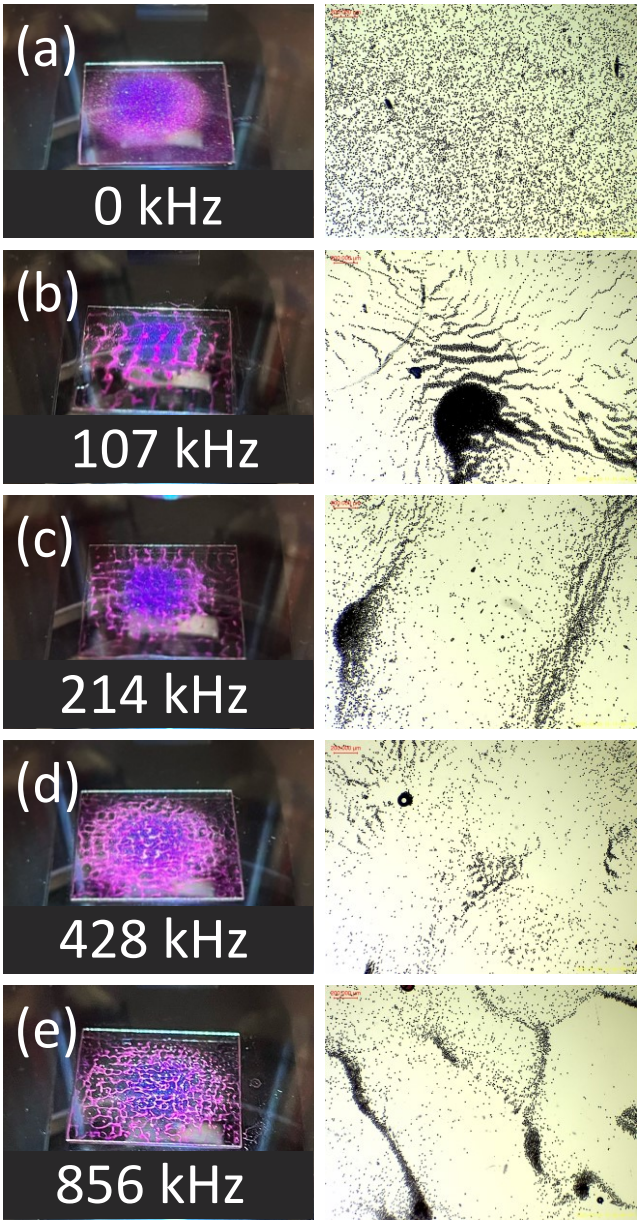

Figure 6. Illustration of patterns formed after 15 minutes of acoustic excitation. The left panels show the patterns as seen by eye and the right panels show the view as seen on the microscope imaged with a microscope camera (magnification ×200). The scale is located at the top left corner of each microscope image. Purple lines indicate PS particles clustering along the pressure nodes while clear spaces indicate the lack of PS particles in antinodes. a) Images taken before acoustic excitation. (b-e) Images taken after 15 minutes of acoustic excitation.

In Figure 6, image (a) (0 kHz), we observed that the particles were well dispersed before the manipulation. In image (b) (107 kHz), the left panel shows that standing wave pattern formed at the manipulation surface, a crude grid-like particle arrangement consisting of approximately

eight horizontal and vertical lines. One of the bulky intersections formed by these lines is visible in the right panel of image (b). As the frequency increases further from images (c) to (e), the observed patterns become more complex and refined. In image (c) (214 kHz) the pattern has become so intricate that two nodal lines can be visible on the microscope in the right panel of image (c). In image (d) (428 kHz) we again see a more intricate grid and on the right panel we can observe an intersection point. In image (e) (856 kHz) we can see that the pattern is the most intricate out of all the frequencies and in the right panel we are able to observe several nodal lines and intersection points.

In our results we can observe that the pattern becomes more complex with the increase of frequency. The increasing complexity of the pattern with the increase in frequency can be observed both on the left panel as progressively thinner lines as well as the microscope images where on the latter frequencies the lines become so thin that they are visible.

6 Discussion

To accurately interpret and analyse the results presented in this thesis, it is essential to first identify the type of acoustic waves that are propagating in our setup. The wave modes present in an acoustic manipulation setup depend on the properties of the substrate through which the waves propagate, the placement and type of transducers that emit the sound waves and the placement and type of the sample, which undergoes acoustic excitation. In similar works the manipulation of particles has been attributed to SAWs, TSAWs, SSAWs, BAWs or flexural waves. Table 1 summarizes these studies providing three examples for each wave mode discussed in this work. The table demonstrates that all of the aforementioned wave modes are capable of patterning, separation and controlled manipulation. To determine which of these wave modes are dominant in our setup we will analyse our setup and experimental observations.

Table 1. Comparison of our work and different acoustic manipulation studies categorized by wave propagation mode, with three examples given for each. Each example includes information on reported application, excitation method, frequency range, solution, substrate and manipulated material.

Wave Type	Application	Excitation Method	Frequency Range	Solution	Substrate	Material	Ref
-	Patterning	Bulk ceramic transducer	107 to 856 kHz	H_2O	Fused quartz	PS particles 10 μm	This work
Flexural waves	Controlled manipulation	Piezoelectric actuator	1.047 to 29.83 kHz	-	Unpolished silicon wafer	Solder balls 600 μm	2
Flexural waves	Patterning	Piezoelectric actuator	1.047 to 29.83 kHz	-	Silicon plate	Solder balls 600 μm	23
Flexural waves	Concentration and separation	Piezoelectric transducer	35 to 50 kHz	H_2O	Glass substrate	PS particles 10 μm	10
SAW	Controlled manipulation	IDT	13.3 MHz	H_2O	Y-128° $LiNbO_3$	PS particles 10 μm	26
SSAW	Patterning	IDT	12.6 to 37 MHz	H_2O	Y-128° $LiNbO_3$	Silver nanowires	11
TSAW	Separation	IDT	97 and 125.5 MHz	H_2O	$LiNbO_3$	PS particles 3 to 10 μm	14
BAW	Controlled manipulation	Bulk ceramic transducer	65 to 700 kHz	H_2O	Fused silica glass	PS particles 70 μm	15
BAW	Patterning and controlled manipulation	Bulk ceramic transducer	65 to 700 kHz	H_2O	Fused silica glass	Water droplets 70, 170 and 500 μm	4
BAW	Separation	Bulk ceramic transducer	2 and 5 MHz	H_2O	Silicon wafer	Red blood cells and cancer cells	16

In Chapter 2 SAWs and their variants were discussed. It was mentioned that in acoustic manipulation research SAWs are generally generated by IDTs. While this is true in the sense that IDTs are highly efficient at generating SAWs the waves can also be excited by other means such as edge reflections and surface scattering. This means that any transducer can generate SAWs albeit inneficiently[27]. Because our system utilizes bulk ceramic transducers, many wave modes including SAWs are generated. However, because our transducers waves scatter along 3D only a fraction of the energy is localized at the surface of our substrate. Due to this fact and

the fact that almost all research regarding acoustic manipulation and the use of SAWs is based on the use of IDTs it is highly unlikely that SAWs, TSAWs or SSAWs are responsible for patterns observed in our setup.

On the other hand, the transducers used in our setup are well equipped to produce BAWs. Bulk ceramic transducers have been used in a myriad of systems, which focus on manipulating particles inside microfluidic channels and chambers located in the bulk of the material[15,16]. However, our setup does not utilize microfluidics nor any kid of a chamber. The mounting of a coverslip sandwiching our sample between two plates creates a chamber-like structure. Nevertheless, our sample is not located within the bulk of our substrate which disqualifies any kind of BAWs to be responsible for the patterning.

By using Equation 3 we can further validate that neither BAWs nor SAWs and their variants are solely responsible for the patterns observed in our experiments. By calculating the wavelength for the first sample as seen in Figure 6 image (b) (107 kHz) using Equation 2 and parameters f = 107 kHz for the frequency and v = 1481 m/s for the velocity of sound in water the wavelength for both BAWs, SAWs and its variants is λ = 13.85 mm. We can calculate the number of nodes that should form on a 18 mm × 18 mm coverslip by using Equation 3. Using Equation 3 where L = 18 mm and λ = 13.85 the number of nodes forming between the glass and the coverslip is N = 2.60. By comparing this result to Figure 6 image (b) (107 kHz) left panel we can see that the calculated N-value does not match the amount of visible nodal lines which is roughly N = 8.

Flexural waves are known to propagate in thin plates under low frequency excitation. Flexural waves can be generated with bulk ceramic transducers, which we used in our setup. However, according to Kirchhoff-Love plate theory flexural waves can only be considered if the wavelength of the acoustic wave is much greater than the thickness of the plate and significantly smaller than the lateral size of the plate as seen in Equation 5. To validate whether flexural waves are responsible for the patterning, we can use Equation 2 to calculate the wavelength for the flexural waves and compare it to the thickness of our substrate in accordance with Equation 5. However, the velocity of the flexural waves would need to be calculated first.

The velocity for flexural waves can be calculated by applying the Kirchhoff-Love phase velocity Equation 4, where the modulus of elasticity E = 74 GPa, plate thickness h = 2 mm, Poisson's Ratio v = 0.17, density of the material ρ = 2200 kg/m^3 and angular frequency ω = $5.25 \cdot 10^6$ rad/s were used[28]. With these parameters we calculated that $v_p \approx 4223.63$ m/s.

By using Equation 2 where $f = 856$ kHz as the highest frequency used in our experiments and velocity of flexural waves $v_p \approx 4223.63$ m/s we calculated that the wavelength $\lambda \approx 4.94$ mm. By applying Equation 5 where wavelength $\lambda \approx 4.94$ mm, length of the plate $L = 75$ mm and plate thickness $h = 2$ mm it is evident that the equation's assumptions are not fulfilled, since the wavelength is not much greater than the plates thickness. Consequently, flexural waves cannot be responsible for patterning in our setup, since they could not have patterned our sample at the frequency of $f = 856$ kHz.

The most important element for analysing our setup is the presence of a thin droplet of fluid, flattened between a 2 mm thick fused quartz substrate and a 0.2 mm thick borosilicate coverslip. This arrangement creates a highly confined, quasi-two-dimensional fluid layer. Under acoustic excitation by two opposing transducers, this suspension layer appears to support standing pressure waves. Similar systems are described in several works, where symmetric grid like patterning is attributed to standing pressure waves confined within a thin fluid layer between two rigid plates[29]. However, in those systems the patterning is achieved in sessile droplets. In spite of that we hypothesize that the same underlying physics concerning standing pressure waves formed by interference also applies to confined fluid layers. In our case pressure waves refer to lateral standing waves in a fluid layer generated by reflections and interference within the thin fluid layer.

In our results we can observe that at the frequency of $f = 107$ kHz approximately eight ($N = 8$) nodal lines form across an 18 mm × 18 mm coverslip. The number of nodal lines seems to double with the doubling of the frequency. This doubling behaviour implies that the nodal lines correspond to half-wavelength spacing of a standing pressure wave. Using this information and utilizing Equation 1 and Equation 2 with parameters $N = 8$ as the number of observed nodes, $L = 18$ mm as the length of the coverslip and $f = 107$ kHz as the frequency we can estimate the acoustic velocity to be $v = 481$ m/s. The calculated speed based on the estimated number of nodes is far too slow for any of the previously proposed wave modes to be responsible for the patterns.

Theoretically the patterns forming on our substrate should be periodic and regular since the transducers are aligned and equally distanced from each other. In practice we observe a grid shape at every frequency. However, the observed patterns were irregular and non-uniform in shape, a feature that becomes especially pronounced every time the frequency is doubled. Due

to this, counting the number of nodal lines gets increasingly harder with the increase of frequency.

The deviations in the patterns can be attributed to many reasons. One of the reasons is the fact that when a coverslip is mounted on top of the droplet, some bubbles and air gaps might get trapped between the coverslip and the fused quartz substrate changing the shape of the acoustic field and introducing capillary forces. In Figure 6 image (d) (428 kHz) right panel a bubble can be observed on the top left corner with PS particles clustering around it. The bubbles explain the ringlike structures visible in our samples.

The placement of the transducer was done within a >1 mm error margin. However, even the slightest deviation between the two transducers will cause the acoustic field to change shape. Furthermore, mounting of the coverslip on top of the sample was done by hand, which introduced variability in alignment between the different samples. Additionally, during acoustic excitation vibration of the substrate caused slight movement of the coverslip, which contributed to the variations in alignment between samples. This likely caused some of the patterns to be slightly slanted to one side.

The varying line thicknesses and gaps in the pattern can be most likely attributed to the PS particle solution being suboptimal. It appears that the concentration of the PS particles was too high causing irregularities in the patterns. Furthermore, given more time under acoustic excitation the PS particles might have migrated more uniformly and formed more consistent patterns.

7 Conclusions

For the purposes of this work, we built an acoustic manipulation setup based on other systems described in literature. We demonstrated the working principle of acoustic manipulation by patterning PS particles suspended in a thin liquid layer. Additionally, we analysed our setup to identify the wave modes responsible for patterning, which revealed deficiencies in our setup and highlighted challenges to be addressed in future work.

The impedance matching transformer was one of the most crucial components in our system. In its absence, impedance mismatch leads to significantly reflective losses sharply reducing power transfer to the transducers. Despite the fact that we were able to match the impedance at the first frequency f = 107 kHz subsequent frequency doubling reintroduced a degree of impedance mismatch albeit significantly reduced compared to the mismatch observed without the transformer. In future work, this challenge can be alleviated by using a switchable high-bandwidth transformer, which can match the impedance at any frequency.

Currently, the setup cannot guide particles along set paths and is completely manually driven. In future work the setup can be further improved by incorporating machine vision in tandem with machine learning to fabricate a smart system, which could tune the signal parameters based on our needs. Machine learning powered system could collect data over several manipulation cycles to both map the acoustic fields formed on the manipulation surface and use that data to move singular or several particles in a controlled manner.

Acoustic manipulation systems like the one we had developed could replace conventional instruments in a wide range of applications. Despite the fact that in this work we exclusively demonstrated patterning, separation can be achieved by using at least two different particles. In addition, controllable manipulation could be achieved by incorporating a machine vision-based smart system. The setup which we built could be well utilized in drug development, health technology and biology applications where handling of cells, proteins and enzymes is of interest.

After analysing our setup, we could not determine a single wave mode responsible for the patterning of the PS particles in our system. To conclude, confirming the type of waves propagating in our system would require validation based on simulations, without which we hypothesize that the waves responsible for the patterns observed in our experiments are standing pressure waves caused by reflections and interference in the thin fluid suspension layer.

References

1. Chladni, E. F. F. *Entdeckungen Über Die Theorie Des Klanges*. (Zentralantiquariat der Deutschen Demokratischen Republik, 1787).
2. Zhou, Q., Sariola, V., Latifi, K. & Liimatainen, V. Controlling the motion of multiple objects on a Chladni plate. *Nat Commun* **7**, 12764 (2016).
3. Bruus, H. Acoustofluidics 7: The acoustic radiation force on small particles. *Lab on a Chip* vol. 12 1014–1021 Preprint at https://doi.org/10.1039/c2lc21068a (2012).
4. Yiannacou, K., Sharma, V. & Sariola, V. Programmable Droplet Microfluidics Based on Machine Learning and Acoustic Manipulation. *Langmuir* **38**, 11557–11564 (2022).
5. Gedge, M. & Hill, M. Acoustofluidics 17: Theory and applications of surface acoustic wave devices for particle manipulation. *Lab on a Chip* vol. 12 2998–3007 Preprint at https://doi.org/10.1039/c2lc40565b (2012).
6. Lenshof, A., Evander, M., Laurell, T. & Nilsson, J. Acoustofluidics 5: Building microfluidic acoustic resonators. *Lab Chip* **12**, 684–695 (2012).
7. Bruus, H. Acoustofluidics 10: Scaling laws in acoustophoresis. *Lab Chip* **12**, 1578–1586 (2012).
8. Bruus, H. Acoustofluidics 7: The acoustic radiation force on small particles. *Lab on a Chip* vol. 12 1014–1021 Preprint at https://doi.org/10.1039/c2lc21068a (2012).
9. Devendran, C., Albrecht, T., Brenker, J., Alan, T. & Neild, A. The importance of travelling wave components in standing surface acoustic wave (SSAW) systems. *Lab Chip* **16**, 3756–3766 (2016).
10. Peng, T., Li, L., Zhou, M. & Jiang, F. Concentration of Microparticles Using Flexural Acoustic Wave in Sessile Droplets. *Sensors* **22**, (2022).
11. Chen, Y. *et al.* Tunable nanowire patterning using standing surface acoustic waves. *ACS Nano* **7**, 3306–3314 (2013).
12. Shi, J. *et al.* Acoustic tweezers: Patterning cells and microparticles using standing surface acoustic waves (SSAW). *Lab Chip* **9**, 2890–2895 (2009).
13. Destgeer, G., Lee, K. H., Jung, J. H., Alazzam, A. & Sung, H. J. Continuous separation of particles in a PDMS microfluidic channel via travelling surface acoustic waves (TSAW). *Lab Chip* **13**, 4210–4216 (2013).
14. Destgeer, G. *et al.* Travelling surface acoustic waves microfluidics. in *Physics Procedia* vol. 70 34–37 (Elsevier, 2015).
15. Yiannacou, K. & Sariola, V. Controlled Manipulation and Active Sorting of Particles Inside Microfluidic Chips Using Bulk Acoustic Waves and Machine Learning. *Langmuir* **37**, 4192–4199 (2021).

16. Augustsson, P., Magnusson, C., Nordin, M., Lilja, H. & Laurell, T. Microfluidic, Label-Free Enrichment of Prostate Cancer Cells in Blood Based on Acoustophoresis. *Anal Chem* **84**, 7954–7962 (2012).
17. Vachon, P. *et al.* Cavity-agnostic acoustofluidic manipulations enabled by guided flexural waves on a membrane acoustic waveguide actuator. *Microsyst Nanoeng* **10**, (2024).
18. Darabi, A., Zareei, A., Alam, M. R. & Leamy, M. J. Broadband Bending of Flexural Waves: Acoustic Shapes and Patterns. *Sci Rep* **8**, (2018).
19. Sky, A., Neunteufel, M., Hale, J. S. & Zilian, A. A Reissner–Mindlin plate formulation using symmetric Hu-Zhang elements via polytopal transformations. *Comput Methods Appl Mech Eng* **416**, (2023).
20. Alexander, C. K. . & Sadiku, M. N. O. . *Fundamentals of Electric Circuits*. (McGraw-hill Education, 2017).
21. David Halliday, R. R. J. W. *Fundamentals of Physics*. (Wiley, 2013).
22. Yiannacou, K. & Sariola, V. Acoustic Manipulation of Particles in Microfluidic Chips with an Adaptive Controller that Models Acoustic Fields. *Advanced Intelligent Systems* **5**, 2300058 (2023).
23. Kopitca, A., Latifi, K. & Zhou, Q. Programmable assembly of particles on a Chladni plate. *Sci Adv* **7**, eabi7716 (2025).
24. Val Baker, A. *et al.* Exploration of Resonant Modes for Circular and Polygonal Chladni Plates. *Entropy* **26**, (2024).
25. Whitesides, G. M. The origins and the future of microfluidics. *Nature* vol. 442 368–373 Preprint at https://doi.org/10.1038/nature05058 (2006).
26. Jo, M. C. & Guldiken, R. Particle manipulation by phase-shifting of surface acoustic waves. *Sens Actuators A Phys* **207**, 39–42 (2014).
27. Namdeo, A. K., Nemade, H. B. & Ramakrishnan, N. *FEM Simulation of Generation of Bulk Acoustic Waves and Their Effects in SAW Devices*.
28. MatWeb. Fused Quartz Material Properties. https://www.matweb.com/search/DataSheet.aspx?MatGUID=ffccd1bca743445ca3bc1706a52974dd&ckck=1 (2025).
29. Friend, J. & Yeo, L. Y. Microscale acoustofluidics: Microfluidics driven via acoustics and ultrasonics. *Rev Mod Phys* **83**, 647–704 (2011).